Research Square

Preprints are preliminary reports that have not undergone peer review.
They should not be considered conclusive, used to inform clinical practice,
or referenced by the media as validated information.

SR-18292 Alters Oocyte Competence and Ovarian Transcriptomic Dynamics in Female Mice

Mandanda N. Mthethwa
National Taiwan University
Giovanny Angelita
National Taiwan University
Yovita Permata Budi
National Taiwan University
En-Tzu Chang
National Taiwan University
Chien Huang
National Taiwan University
Chih-Hsien Chiu
National Taiwan University
Yi-Fan Jiang
yfjiang@ntu.edu.tw

National Taiwan University

Research Article

Keywords: SR-18292, mitochondrial biogenesis, PGC-1α, estrous cycle, ovarian transcriptome, oocyte competence, superovulation, in vitro fertilization

Posted Date: November 13th, 2026

DOI: https://doi.org/10.21203/rs.3.rs-11710370/v1

License: This work is licensed under a Creative Commons Attribution 4.0 International License.
Read Full License

Additional Declarations: No competing interests reported.

Abstract

Background

Mitochondria are essential for ovarian function, steroidogenesis, and oocyte development. However, the role of mitochondrial biogenesis in estrous cyclicity and oocyte competence remains incompletely understood. This study investigated the effects of SR-18292-mediated peroxisome proliferator-activated receptor gamma coactivator 1-alpha (PGC-1α) inhibition on reproductive outcomes and ovarian transcriptomic profiles in female ICR mice.

Methods

Estrous cyclicity was monitored before, during, and after SR-18292 treatment. Oocyte yield, degeneration, and fertilization outcomes were evaluated following gonadotropin-induced superovulation and in vitro fertilization (IVF). Ovarian transcriptomes were analyzed by RNA sequencing at 48 h after pregnant mare serum gonadotropin (PMSG) and 13 h after human chorionic gonadotropin (hCG) administration, followed by differential gene expression and pathway enrichment analyses.

Results

SR-18292 treatment disrupted estrous cyclicity, with prolonged or stalled progression at metestrus and diestrus. Treated mice yielded significantly more ovulated oocytes following superovulation, but these oocytes exhibited a greater degeneration rate and almost no successful fertilization compared to the control group. Transcriptomic changes were more pronounced 13 h after hCG than 48 h after PMSG administration. Early transcriptomic responses were associated primarily with activated lipid metabolism, adipocytokine signaling, and hormone-related processes. Moreover, later transcriptomic responses included suppression of mitochondrial respiratory-chain and oxidative phosphorylation-associated gene categories, alongside alterations in metabolic and signaling pathways.

Conclusions

SR-18292 treatment was associated with disrupted estrous cyclicity, increased ovulatory output, and impaired oocyte competence. Transcriptomic analysis suggests that metabolic, hormone-responsive, and energy-sensing pathways may sustain follicular development and ovulation despite pharmacological modulation of PGC-1α, yet fail to preserve oocyte competence, revealing a potential uncoupling between ovulatory output and oocyte developmental potential. These findings support further investigation into the role of PGC-1α-associated mitochondrial regulation in female reproduction.

Introduction

Follicular development and oocyte maturation are closely coordinated processes that determine female reproductive competence. During folliculogenesis, granulosa and theca cells undergo dynamic changes in response to gonadotropins and intraovarian signaling, supporting follicular growth, steroidogenesis, and ovulation (1–4). Oocytes also depend on metabolic cooperation with surrounding granulosa and cumulus cells, which provide essential substrates and signaling molecules through gap junctions and transzonal projections (5–7). Oocyte development involves cytoplasmic remodeling, accumulation of organelles and maternal RNAs, and acquisition of the molecular components required to support fertilization, implantation, early embryogenesis, and subsequent pregnancy outcomes (8, 9). Among the cellular components involved in this process, mitochondria play a particularly important role in supporting oocyte development and maturation. Beyond ATP production through oxidative phosphorylation (OXPHOS), mitochondria regulate calcium homeostasis, redox balance, and cellular signaling, all of which contribute to oocyte quality and developmental potential (10–15). Mitochondrial activity is closely associated with meiotic progression, chromosome segregation, and early embryonic development, whereas excessive reactive oxygen species (ROS) and mitochondrial dysfunction can compromise oocyte maturation and fertilization (14–16). These findings highlight the importance of mitochondrial function in maintaining reproductive competence.

Mitochondrial function is maintained through coordinated regulation of mitochondrial biogenesis, dynamics, and quality control. Peroxisome proliferator-activated receptor gamma coactivator 1-alpha (PGC-1α) is a major transcriptional coactivator involved in mitochondrial biogenesis through the regulation of nuclear respiratory factors and other transcriptional regulators of mitochondrial function (17–19). Mitochondrial dynamics, including fusion and fission, further allow organelles to adapt their morphology, distribution, and functional capacity to changing cellular demands (20, 21). These processes are particularly relevant to ovarian physiology, in which metabolic requirements change throughout follicular development, ovulation, luteinization, and corpus luteum formation (5, 22, 23). Hormonal stimulation may therefore influence ovarian mitochondrial activity through changes in mitochondrial regulatory pathways and broader metabolic transcriptional networks. Nevertheless, how these regulatory processes contribute to ovarian cyclicity, ovulatory function, and oocyte developmental competence remains incompletely understood.

Previous studies have provided evidence linking mitochondrial remodeling to ovarian reproductive physiology. In our previous studies, we demonstrated stage-dependent changes in mitochondrial morphology and distribution during goat corpus luteum development (23). We also showed that treatment with the mitochondrial fusion promoter M1 disrupted estrous cycle dynamics and altered mitochondrial respiratory complex expression in female mice (24). These findings suggest that mitochondrial regulation is involved in ovarian function, but the consequences of manipulating mitochondrial biogenesis-related pathways for ovulation and oocyte competence remain unclear. In addition, the accompanying ovarian transcriptional responses, particularly those associated with metabolic adaptation and mitochondrial function during gonadotropin-induced follicular development and ovulation, have not been fully characterized.

SR-18292 is a small molecule originally identified as an inhibitor of PGC-1α-dependent transcriptional activity through increased PGC-1α acetylation (18). Although its direct molecular target has not been fully established, SR-18292 provides a pharmacological approach to investigate the consequences of reduced PGC-1α activity in vivo (18, 25). In the present study, we investigated the effects of SR-18292 treatment on estrous cycle progression, ovulatory output, and oocyte developmental competence in female mice. We further characterized ovarian transcriptomic responses at two stages of gonadotropin stimulation, following PMSG and hCG administration, to identify changes in metabolic pathways, mitochondrial function, and associated biological processes. By integrating reproductive phenotypes with transcriptomic analysis, this study aimed to provide insight into how PGC-1α-associated mitochondrial regulation may influence ovarian function and the relationship between ovulatory activity and oocyte developmental potential.

Materials and Methods

Animals

Female ICR mice aged 10 weeks or ~ 5 weeks and male ICR mice aged 10–12 weeks were obtained from BioLASCO, Taiwan. All mice were maintained under controlled temperature and humidity conditions with a 12-h light/dark cycle and had ad libitum access to food and water. Ten-week-old female mice were used for estrous cycle monitoring and in vitro fertilization (IVF) experiments, whereas approximately 5-week-old female mice were used for transcriptomic analysis. Male mice were housed in the same room as the females to help maintain regular estrous cycles (26). All animal procedures were conducted in accordance with the Guide for the Care and Use of Laboratory Animals (National Institutes of Health, NIH Publication No. 80 – 23, revised 1978) and were approved by the National Taiwan University Institutional Animal Care and Use Committee (NTU-108-EL-00112, NTU-113-EL-00154, and NTU-114-EL-00166).

Cycle determination and SR-18292 treatment

Vaginal smears were collected daily from female mice by introducing and aspirating 100 μL of saline into the vaginal canal until an opaque cell suspension was obtained. The suspension was spread onto glass slides and dried on a heating plate. The smears were stained with 0.02% methylene blue, gently rinsed with running water, and examined under a microscope. Estrous cycle stages were determined based on the relative proportions of nucleated epithelial cells, leukocytes, and cornified epithelial cells (27, 28).

22.5 mg/kg BW of SR-18292 (Sml2146, Sigma-Aldrich) was prepared the same way as in previous studies; it was diluted in 5%DMSO, 10% Tween 80, and 85% 1x PBS (18, 24). On the first morning of treatment, vaginal smears were collected to confirm proestrus. SR-18292 (0.3 mL) was administered by injection, followed by vaginal smear collection at noon to monitor estrous cycle changes. A second injection (0.3 mL) was administered at 3:00 p.m. Treatments were continued for five consecutive days.

Superovulation and In Vitro Fertilization (IVF)

For superovulation, female mice aged 10 weeks or ~ 5 weeks were primed intraperitoneally (IP) with 5IU pregnant mare serum gonadotropin (PMSG) (PROSPEC #hor-272-a), with or without SR-18292, followed by 10IU human chorionic gonadotropin (hCG) (Sigma #9002-61-3), with or without SR-18292 after 48 h. Oocytes collected from 10-week-old mice were used for in vitro fertilization (IVF), whereas ovarian tissues from ~ 5-week-old mice were preserved in RNAlater for transcriptomic sequencing. Following treatment, mice were anesthetized via IP injection of 2.5% avertin (0.15 mL/10 g body weight) and euthanized by cervical dislocation.

IVF was performed using a modified protocol described by Taft (2017b) (29). 13 h post- hCG administration, female mice were euthanized, and the oviducts were collected. Cumulus–oocyte complexes (COCs) were released from the ampullae and transferred into prewarmed modified Dulbecco's phosphate-buffered saline (EmbryoMax®, #MR-006-C). Fertilization and sperm collection dishes were prepared in advance using human tubal fluid (HTF; EmbryoMax®, #MR-070-D-1EA) covered with mineral oil and equilibrated at 37°C under 5% CO_2. Cauda epididymides and vasa deferentia were collected from male mice, and sperm were released from the cauda epididymides by making several incisions with a 25-gauge needle. Sperm were incubated for 1 h to allow capacitation. COCs were then transferred into 500-μL HTF drops, and sperm were added to achieve a final concentration of 1–2.5 × 10^6 sperm/mL. Gametes were co-incubated for 4–6 h at 37°C under 5% CO_2. Following insemination, oocytes were washed through sequential HTF drops to remove excess sperm and debris, then incubated overnight. The following morning, oocytes and embryos were examined microscopically. The numbers of ovulated oocytes and degenerated oocytes were recorded, and fertilization success was calculated as the percentage of total oocytes that developed into two-cell embryos.

RNA extraction, quantification and qualification

RNA extraction and quantification for transcriptome sequencing were performed by Biotools (Taiwan). A pair of ovaries was collected from each individual, then subjected to RNA extraction, and the extracts were quantified and checked for purity using SimpliNano™ -Biochrom Spectrophotometers (Biochrom, MA, USA), and Qsep 100 DNA/RNA Analyzer (BiOptic Inc., Taiwan).

Library preparation and transcriptome sequencing

RNA sequencing libraries were prepared using 1 μg of total RNA per sample and the KAPA mRNA HyperPrep Kit (KAPA Biosystems, Roche, Basel, Switzerland), following the manufacturer's instructions. Briefly, mRNA was enriched using magnetic oligo-dT beads, fragmented, and reverse-transcribed into cDNA. Strand-specific libraries were generated through second-strand synthesis incorporating dUTP, followed by adapter ligation and size selection targeting 300 ~ 400 bp fragments using KAPA Pure Beads. Libraries were amplified using KAPA HiFi HotStart ReadyMix and purified with KAPA Pure Beads.

Library quality and quantity were assessed using a Qsep 100 DNA/RNA Analyzer (BiOptic Inc., Taiwan), Qubit 2.0 Fluorometer (Thermo Fisher Scientific), and Agilent Bioanalyzer 2100 system. Sequencing was performed on an Illumina NovaSeq X platform, generating 150-bp paired-end reads.

Data analysis

Raw sequencing reads in FASTQ format were assessed using FastQC and MultiQC (30). Adapter sequences and low-quality reads and bases were removed using Trimmomatic (v0.38) (31). The resulting clean reads were aligned to the mouse reference genome (GRCm38) using HISAT2 (v2.1.0) (32, 33), and gene-level read counts were generated using featureCounts (v2.0.0). Differential gene expression analysis and principal component analysis (PCA) comparing the SR-18292-treated and control groups were performed using DESeq2 (v1.26.0) (34, 35). *P*-values were adjusted using the Benjamini–Hochberg method to control the false discovery rate (FDR). Genes with an adjusted *P*-value < 0.05 and a fold change > 1.5 were considered differentially expressed genes (DEGs). Gene Ontology (GO) and Kyoto Encyclopedia of Genes and Genomes (KEGG) pathway enrichment analyses were performed using clusterProfiler (v3.14.3) (36–38). Gene Set Enrichment Analysis (GSEA) was conducted with 1,000 permutations to identify enriched metabolic pathways using the Gene Set Knowledgebase (GSKB) (39).

Statistical Analysis

Data are presented as the mean ± standard deviation (SD) for IVF outcomes. Differences between groups were analyzed using Student's *t*-test or analysis of variance, as appropriate. A *P*-value < 0.05 was considered statistically significant.

Results

SR-18292 disrupts the estrous cycle

We first investigated the effect of SR-18292, a pharmacological inhibitor of PGC-1α activity, on the estrous cycle in 10-week-old ICR female mice. The mice were treated twice daily for five consecutive days, while their estrous cycles were monitored by vaginal smears before, during, and after the treatment period to assess recovery (Fig. 1A). The control group exhibited a normal sequential progression through proestrus, estrus, metestrus, and diestrus. In contrast, the SR-18292-treated group showed disruption of normal cycle progression, with cycles becoming prolonged or stalling at the metestrus and diestrus stages (Fig. 1B).

Increased ovulation does not preserve oocyte competence

In vitro fertilization (IVF) was performed to evaluate the effects of SR-18292 treatment on oocyte quality and fertilization success. Initially, two doses of SR-18292, 2.25 mg/kg body weight (data not shown as there was no significant difference) and 22.5 mg/kg body weight (used throughout the study), were tested to evaluate the treatment response. For each treatment and control group, three 10-week-old

female ICR mice underwent superovulation induced by sequential administration of pregnant mare serum gonadotropin (PMSG) and human chorionic gonadotropin (hCG) as shown in Fig. 2A. Following ovulation, cumulus–oocyte complexes (COCs) were collected from the oviducts. The COCs were subsequently inseminated with capacitated sperm in fertilization medium under sterile conditions to initiate the fertilization process. Following IVF, the cumulus cells detached from the oocytes, allowing the ovulated oocytes to be counted. Representative images of oocytes from the control group are shown in Fig. 2B (upper panel). Post-fertilization, the extruded polar body was observed in the control oocytes (Fig. 2B, upper left panel), and after overnight incubation, embryos at the 2-cell stage were observed (Fig. 2B, upper right panel). A substantial proportion of the retrieved oocytes exhibited morphological degeneration (Fig. 2B, lower left panel) and failed to undergo fertilization (Fig. 2B, lower right panel) from the SR-18292-treated mice. The SR-18292-treated group yielded a significantly higher number of oocytes compared with the control group (Fig. 2C). Although the SR-18292-treated group ovulated significantly more oocytes than the control group, the quality of the retrieved oocytes was markedly reduced. This reduction in oocyte quality was reflected in the fertilization rate, which was substantially lower in the SR-18292-treated group than in the control group (Fig. 2D). Furthermore, the oocyte degeneration rate was significantly higher following SR-18292 treatment compared with the control group (Fig. 2E). Collectively, these findings demonstrate that SR-18292 treatment increased the number of ovulated oocytes but substantially reduced their developmental competence, as evidenced by increased oocyte degeneration and decreased fertilization success.

RNA-sequencing reveals distinct ovarian transcriptomic responses to SR-18292 exposure

Next-generation sequencing (NGS) was performed to characterize dynamic changes in gene expression and biological pathways during superovulation, with and without SR-18292 treatment. The experimental design is outlined in Fig. 3A. Ovarian samples were collected from ~ 5-week-old mice at two time points: 48 h after PMSG administration (TreatA and ControlA), representing the follicular development stage, and 13 h after hCG administration (TreatB and ControlB), following the ovulatory event. Two-dimensional principal component analysis (PCA) revealed distinct clustering among biological replicates within each experimental group (ControlA, TreatA, ControlB, and TreatB), with relatively low variation among samples collected at the same time point (Fig. 3B). These results indicate good consistency among biological replicates and demonstrate separation between treatment and control groups. Based on the PCA distribution, differentially expressed genes (DEGs) were identified using an adjusted *P*-value < 0.05 and a fold change > 1.5 as the filtering criteria. Volcano plots were generated to visualize gene expression changes between SR-18292-treated and control groups at each sampling time point. TreatA versus ControlA showed fewer transcriptional changes, with 24 significantly upregulated genes and 10 significantly downregulated genes (Fig. 3C). In contrast, a greater number of transcriptional changes was observed in TreatB versus ControlB, corresponding to the post-ovulatory sampling time point. In this comparison, 225 genes were significantly downregulated, whereas 156 genes were significantly upregulated (Fig. 3D). The differences in the number and direction of DEGs between the two time points

may reflect differences in the ovarian physiological state associated with follicular development and the post-ovulatory period, as well as the temporal effects of SR-18292 treatment. Collectively, these results demonstrate that SR-18292 treatment was associated with more pronounced transcriptomic changes at 13 h after hCG administration than at 48 h after PMSG administration, suggesting that the ovarian transcriptional response to SR-18292 treatment differed between the follicular development and post-hCG stages.

Alternative metabolic and endocrine pathways may support follicular development

We next performed gene set enrichment analysis (GSEA) of the TreatA and ControlA datasets to characterize the functional categories further and signaling pathways associated with SR-18292 treatment. Following selection of the top 10 enriched pathways, several of the positively enriched pathways were associated with lipid metabolism, whereas negatively enriched pathways included sensory-related and G protein-coupled receptor signaling pathways (Fig. 4A). Figure 4B presents the top 10 positively enriched signaling pathways, including hormone-related signaling, AMPK, adipocytokine, and glucagon signaling pathways. We subsequently examined heatmaps to identify individual genes contributing to the enriched pathways and to compare their expression patterns between the SR-18292-treated and control groups. In the hormone activity heatmap, TreatA mice exhibited higher expression of several genes, including *Adipoq*, *Lep*, and *Retn*, compared with ControlA mice (Fig. 4C). The ovulation cycle process heatmap showed increased expression of genes such as *Lep* and *Lhcgr* in TreatA mice (Fig. 4D). Collectively, these findings provide an overall enrichment of pathways following early exposure to SR-18292 was associated with changes in metabolic and hormone-related transcriptional programs, and show limited suppressed pathways when filtered to show the top 10 enriched pathways.

Early SR-18292 exposure induces compensatory metabolic and hormone-responsive transcriptional pathways

To characterize the functional categories represented by the differentially expressed genes, the top 15 Gene Ontology (GO) terms were analyzed using a fold-change threshold of > 1.5 and an adjusted *P*-value < 0.05. The majority of the enriched genes in TreatA were upregulated compared with ControlA, with prominent GO categories including acylglycerol metabolic process, neutral lipid metabolic process, fatty acid catabolic process, and cellular response to peptide, each involving approximately four to five genes (Fig. 5A). In contrast, only a small number of genes were downregulated, ranging from zero to two genes across the identified GO categories. Upregulation of genes involved in the cellular response to peptide hormone stimulus was also observed, suggesting altered hormone- and peptide-responsive transcriptional activity following SR-18292 treatment (Fig. 5B). Consistent with these findings, the heatmap demonstrated an overall increase in genes associated with the positive regulation of lipid localization in TreatA compared with ControlA (Fig. 5C). The AMPK signaling pathway was positively enriched in the treated group, as indicated by the heatmap, with several genes showing increased

expression (Fig. 5D). This pattern may reflect altered metabolic transcriptional programs that could contribute to maintaining cellular energy homeostasis under conditions of altered mitochondrial function.

Superovulation reveals altered ovarian transcriptional pathways associated with mitochondrial function

We next investigated the effects of SR-18292 treatment following superovulation by comparing the TreatB and ControlB groups. First, GO analysis was performed to characterize the functional categories represented among the differentially expressed genes. Among the top 15 enriched GO terms, downregulated genes were predominantly associated with calcium ion concentration and calcium homeostasis, whereas upregulated genes were enriched in processes related to heart contraction and peptide receptor activity (Fig. 6A). We subsequently performed GSEA to further characterize the biological pathways affected after SR-18292 treatment. Several mitochondrial-related pathways were negatively enriched in TreatB, including NADH dehydrogenase complex assembly, mitochondrial respiratory complex, and mitochondrial membrane protein-related pathways (Fig. 6B).

In contrast, positively enriched pathways included the MAPK cascade, protein kinase activity, cell-surface signaling, and cytokine production. Oxidative phosphorylation was also negatively enriched following SR-18292 treatment, whereas steroid hormone biosynthesis, lipolysis in adipocytes, and adipocytokine signaling were positively enriched (Fig. 6C). In the dot plots, dot color represents the adjusted *P*-value, while dot size indicates the number of genes contributing to each pathway. The enrichment plots provided further insight into the distribution of genes within selected pathways. The hormone-related heatmap showed increased expression of several genes in the SR-18292-treated group, indicating alterations in hormone-associated transcriptional responses (Supplementary Fig. 1B). The mitochondrial respiratory chain complex and cytosolic large ribosomal subunit pathways showed enrichment patterns concentrated toward the right side of the plots, indicating that a substantial proportion of genes within these pathways were downregulated in the SR-18292-treated group and relatively enriched in the control group (Fig. 6D and Supplementary Fig. 1A, respectively). Collectively, these transcriptomic findings indicate that SR-18292 treatment following superovulation is associated with substantial alterations in mitochondrial-related pathways, particularly those involved in mitochondrial respiratory complex function and oxidative phosphorylation. These results provide molecular evidence supporting an association between reduced PGC-1α-dependent transcriptional activity and altered ovarian mitochondrial-related transcriptional responses following superovulation.

SR-18292 differentially regulates mitochondrial, ribosomal, and steroidogenic gene expression following superovulation

Moreover, Fig. 7A and Fig. 7B custom heatmaps show representative downregulated TreatB genes selected based on overall fold change in mitochondrial and ribosomal categories, respectively. Briefly, GSEA data tables were used for the respective categories, and genes were sorted according to absolute fold change from the most negative to closest to zero. Genes from the selected categories were plotted in the heatmaps. Additionally, adipocytokine signaling (Fig. 7C) and steroid hormone biosynthesis (Fig. 7D) were positively enriched in the SR-18292-treated groups, although some variation in gene expression was observed among biological replicates within each group. Notably, *Lep*, *Pck1*, and *Adipoq* were consistently upregulated in both TreatA and TreatB across the pathway analyses.

Collectively, these results suggest that SR-18292 treatment is associated with increased activity of lipid metabolism, AMPK signaling, steroid hormone biosynthesis, and adipocytokine-related transcriptomic responses. These transcriptional changes suggest that SR-18292 treatment was associated with alterations in lipid metabolism, AMPK-associated signaling, steroid hormone biosynthesis, and adipocytokine-related pathways, alongside suppression of mitochondrial respiratory chain and oxidative phosphorylation-related genes. Whether these changes represent compensatory responses that help maintain ovarian function under altered mitochondrial conditions remains to be determined. Further functional studies will be required to determine whether these transcriptional changes directly contribute to the maintenance of ovarian function under mitochondrial stress.

Discussion

The present study demonstrates that pharmacological modulation of PGC-1α activity by SR-18292 affects ovarian reproductive function at both the cyclic and superovulatory levels. SR-18292 treatment disrupted estrous cycle progression and, unexpectedly, increased the number of oocytes retrieved following gonadotropin-induced superovulation while markedly reducing their fertilization competence. Transcriptomic analysis further revealed distinct ovarian responses at the PMSG and hCG stages, with changes in metabolic and hormone-associated pathways at the earlier stage and more extensive alterations in mitochondrial respiratory chain and oxidative phosphorylation-related gene sets at the later stage. Together, these findings suggest that ovarian activity and oocyte developmental competence may respond differently to perturbations in PGC-1α-associated regulation.

The disruption of estrous cycle progression following SR-18292 treatment suggests that PGC-1α-associated pathways contribute to the maintenance of normal ovarian cyclicity. The prolonged or stalled progression observed predominantly at metestrus and diestrus indicates that the effects of treatment may extend beyond a transient disturbance of a single cycle. Normal ovarian cyclicity requires coordinated changes in follicular development, steroidogenesis, ovulation, and corpus luteum function, all of which involve substantial metabolic and mitochondrial regulation (13, 40). PGC-1α has also been implicated in ovarian steroidogenic activity through interactions with transcriptional regulators such as steroidogenic factor-1 and liver receptor homolog-1, which are involved in the regulation of steroidogenic genes and progesterone production in granulosa cells (41). Thus, altered PGC-1α activity may influence estrous cycle progression through changes in ovarian metabolism and endocrine function. Nevertheless,

SR-18292 was originally characterized as a pharmacological inhibitor of PGC-1α-dependent transcription through increased PGC-1α acetylation and altered interaction with GCN5 (18, 25). Its effects should therefore not be attributed exclusively to mitochondrial biogenesis. The present findings are consistent with a role for PGC-1α-associated regulation in ovarian cyclicity, although further studies using genetic or complementary pharmacological approaches are needed to establish the specific mechanisms involved.

One of the most notable findings was the apparent dissociation between ovulatory output and oocyte competence. Despite the disruption of estrous cyclicity, SR-18292-treated mice yielded significantly more oocytes following superovulation than control mice. However, these oocytes exhibited increased degeneration and substantially reduced fertilization success. This result indicates that a greater number of recovered oocytes does not necessarily reflect improved reproductive function. Mitochondria are essential for oocyte maturation and early embryonic development because of their roles in ATP production, calcium regulation, and redox homeostasis (13, 40, 42, 43). Mitochondrial number, distribution, and activity also undergo dynamic changes during oocyte growth and maturation, and mitochondrial abnormalities have been associated with reduced developmental competence (44, 45). Consequently, ovarian processes sufficient to support follicular development and ovulation may not necessarily provide the metabolic and cellular conditions required for successful oocyte maturation and fertilization. This distinction may be particularly important during gonadotropin-induced superovulation, in which follicular recruitment and ovulatory responses are strongly stimulated. The increased oocyte yield observed in the present study may therefore represent preserved or enhanced ovulatory responsiveness despite compromised oocyte quality. Previous studies have linked mitochondrial dysfunction to impaired oocyte development through changes in ATP availability, oxidative stress, calcium homeostasis, membrane potential, and mitochondrial quality control (46, 47). Although the present study did not directly measure these parameters in individual oocytes, the increased degeneration and reduced fertilization rate provide functional evidence of impaired oocyte competence following SR-18292 treatment. The precise mitochondrial mechanisms underlying this phenotype remain to be determined.

The ovarian transcriptomic responses differed between the two sampling stages. At 48 h after PMSG administration, relatively few differentially expressed genes were identified, and the enriched pathways were predominantly associated with lipid metabolism, adipocytokine signaling, AMPK-associated processes, and hormone-related responses. These findings suggest that the ovarian response during follicular development involved changes in metabolic and endocrine-associated transcriptional programs rather than widespread suppression of mitochondrial-related gene expression. Lipid metabolism is particularly relevant to ovarian function because lipids provide substrates for energy metabolism and precursors for steroid hormone synthesis, in addition to participating in cellular signaling (48, 49). The enrichment of AMPK-associated pathways is also noteworthy, given the established role of AMPK in cellular energy homeostasis and its involvement in follicular development, oocyte maturation, and ovarian steroidogenesis (50, 51). AMPK-related signaling has further been associated with steroidogenic regulation in granulosa cells (52, 53). These transcriptional changes may reflect an ovarian response to altered metabolic conditions following SR-18292 treatment. However,

pathway enrichment does not establish increased AMPK activity or demonstrate that these responses functionally compensate for mitochondrial perturbation.

Among the genes repeatedly identified in the metabolic and adipocytokine-related analyses, *Lep* was particularly notable, appearing in multiple pathway-associated heatmaps across the two sampling stages. The expression patterns of *Adipoq*, *Retn*, and *Pck1* further suggest that adipokine-related and metabolic transcriptional responses were affected by SR-18292 treatment. This observation is of potential reproductive relevance because leptin links metabolic status to the hypothalamic–pituitary–gonadal axis and may also influence ovarian function (54, 55). Previous studies have demonstrated the expression of leptin and its receptors in granulosa and cumulus cells and have reported direct effects of leptin on ovarian steroidogenesis (56–58). In particular, the repeated appearance of *Lep* suggests that leptin-associated signaling may be a relevant candidate for further investigation at the interface between ovarian metabolism and reproductive function. Nevertheless, the present whole-ovary transcriptomic analysis cannot identify the cellular sources of these transcripts or establish changes in leptin production, circulating leptin concentrations, or downstream signaling activity. Therefore, the contribution of leptin-associated regulation to the observed reproductive phenotype remains an open question.

In contrast to the relatively limited transcriptional changes observed at the PMSG stage, the comparison at 13 h after hCG administration revealed more extensive alterations, particularly the downregulation of gene sets associated with mitochondrial respiratory complexes and oxidative phosphorylation. These findings are consistent with the role of PGC-1α as a major regulator of mitochondrial metabolism and provide evidence that mitochondrial-associated transcriptional programs are affected following SR-18292 treatment during the hCG-induced ovulatory stage. The enrichment of calcium-related gene categories also suggests that calcium-associated processes may be altered. Mitochondria contribute to intracellular calcium buffering and homeostasis (59), while calcium signaling is essential for oocyte maturation, fertilization, and early embryonic development (60, 61). However, because calcium dynamics were not directly assessed in this study, the relationship between the observed transcriptional changes and calcium regulation remains speculative. In addition to mitochondrial-related pathways, the downregulation of genes associated with the cytosolic large ribosomal subunit suggests that protein synthesis-related transcriptional programs may also be affected at this stage. Given the close relationship between cellular energy availability and protein synthesis, this finding may indicate broader changes in cellular metabolic regulation following SR-18292 treatment. However, altered ribosomal gene expression does not necessarily indicate reduced protein synthesis, and further functional analysis would be required to establish its significance.

Taken together, the transcriptomic findings suggest that the ovarian response to SR-18292 differs between follicular development and the hCG-induced ovulatory stage. Changes in lipid metabolism, AMPK-associated signaling, and adipokine-related pathways were already evident at the earlier stage, whereas suppression of mitochondrial respiratory chain and oxidative phosphorylation-related gene sets became more prominent at the later stage. One possible interpretation is that ovarian tissue retains

some capacity to adjust its metabolic and hormone-associated transcriptional programs under altered PGC-1α activity, while mitochondrial-associated processes become more extensively affected during the later phase of gonadotropin stimulation. Such responses may help explain why increased oocyte recovery can occur despite reduced oocyte competence. However, whether the observed metabolic changes represent functional compensation, and whether they directly contribute to the preservation of follicular development or ovulation, remains to be established. More broadly, these findings emphasize that ovulatory output and oocyte developmental potential are distinct reproductive outcomes and should not be considered interchangeable measures of ovarian function. This distinction may also be relevant to assisted reproductive technologies, in which successful oocyte recovery must ultimately be evaluated in relation to fertilization and subsequent developmental competence (62).

Limitations

Several limitations should be considered when interpreting the present findings. First, SR-18292 is a pharmacological modulator of PGC-1α-dependent transcription, and its effects may extend beyond mitochondrial biogenesis. Further studies using genetic approaches or complementary pharmacological strategies are required to establish the specific contribution of PGC-1α-associated regulation. Second, transcriptomic sequencing was performed using whole ovarian tissue, which contains multiple cell populations whose relative abundance and transcriptional states change during follicular development and ovulation. Cell-type-specific or single-cell approaches would help identify the cellular origins of the observed transcriptional responses. Third, mitochondrial function was not directly assessed in individual oocytes. Measurements of ATP production, reactive oxygen species, mitochondrial membrane potential, and mitochondrial DNA integrity would help clarify the relationship between altered mitochondrial regulation and impaired oocyte competence. Finally, the functional significance of the enriched metabolic and hormone-associated pathways remains uncertain because AMPK activity, steroid hormone production, adipokine levels, and protein synthesis were not directly measured. These limitations should be addressed in future studies to determine whether the transcriptional changes identified here represent functional adaptations to altered mitochondrial regulation.

Conclusions

In conclusion, SR-18292 treatment disrupted estrous cycle progression and increased oocyte recovery following superovulation, but this increase was accompanied by greater oocyte degeneration and reduced fertilization success. Ovarian transcriptomic analysis revealed stage-dependent changes in metabolic, hormone-associated, mitochondrial, and ribosomal gene expression. These findings suggest that increased ovulatory output can coexist with impaired oocyte developmental competence following pharmacological modulation of PGC-1α-associated pathways. The results highlight the importance of evaluating oocyte quality in addition to ovulatory output when assessing the reproductive consequences of altered ovarian mitochondrial regulation.

Abbreviations

PGC
1α-peroxisome proliferator-activated receptor gamma coactivator 1-alpha
IVF
in vitro fertilization
PMSG
pregnant mare serum gonadotropin
hCG
human chorionic gonadotropin
FSH
follicle-stimulating hormone
LH
luteinizing hormone
OXPHOS
oxidative phosphorylation
ROS
reactive oxygen species
RNA
seq-RNA sequencing
NRF1
nuclear respiratory factor 1
NRF2
nuclear respiratory factor 2
DEGs
differentially expressed genes
GSEA
gene set enrichment analysis
KEGG
Kyoto Encyclopedia of Genes and Genomes
PCA
principal component analysis
GO
Gene Ontology
GSKB
gene set knowledge base
HTF
human tubal fluid
COCs
cumulus-oocyte-complexes

NGS
next-generation sequencing
PBS
phosphate-buffered saline
DMSO
dimethyl sulfoxide

Declarations

Ethics approval and consent to participate

All animal procedures conducted were reviewed and approved by the National Taiwan University Institutional Animal Care and Use Committee (NTU-108-EL-00112, NTU-113-EL-00154, and NTU-114-EL-00166).

Consent for publication:

Not applicable

Competing interests

The authors declare that they have no competing interests.

Authors' information

Department of Veterinary Medicine, School of Veterinary Medicine, National Taiwan University, Taipei, 10617, Taiwan

Mandanda N. Mthethwa

Graduate Institute of Molecular and Comparative Pathobiology, School of Veterinary Medicine, National Taiwan University, Taipei, 10617, Taiwan

School of Veterinary Medicine, National Taiwan University, Taipei, 10617, Taiwan

Mandanda N. Mthethwa, Yovita Permata Budi, & Yi-Fan Jiang

Department of Animal Science and Technology, National Taiwan University, Taipei, 10617, Taiwan

Chien Huang & Chih-Hsien Chiu

Funding

This work was supported by grants from the Ministry of Science and Technology (109-2320-B-002 -038 -MY3 and 115-2320-B-002-044 -), Taiwan.

Author Contribution

M.N.M., G.A., and Y.-F.J. contributed to conceptualization and methodology. M.N.M., G.A., Y.P.B., and E.-T.C. performed the investigation. Y.-F.J. provided supervision and project administration. C.H. and C.-H.C. contributed reagents and analytical tools. M.N.M., G.A., and Y.-F.J. contributed to data analysis. M.N.M. prepared the original manuscript draft. M.N.M. and Y.-F.J. contributed to writing, reviewing, and editing the manuscript. All authors read and approved the final manuscript.

Acknowledgement

The authors thank Dr. Li-Ying Sung of the Institute of Biotechnology, National Taiwan University, Taipei 10617, Taiwan, for her valuable guidance on the IVF procedures.

Data Availability

All data generated and analyzed in this study are included in this article. Further inquiries may be directed to the corresponding author.

References

1. Dalbies-Tran R, Cadoret V, Desmarchais A, Elis S, Maillard V, Monget P et al. A Comparative Analysis of Oocyte Development in Mammals. Cells. 2020;9(4).
2. Rao MC, Midgley AR Jr., Richards JS. Hormonal regulation of ovarian cellular proliferation. Cell. 1978;14(1):71–8.
3. Almansa-Ordonez A, Bellido R, Vassena R, Barragan M, Zambelli F. Oxidative Stress in Reproduction: A Mitochondrial Perspective. Biology (Basel). 2020;9(9).
4. Das M, Sauceda C, Webster NJG. Mitochondrial Dysfunction in Obesity and Reproduction. Endocrinology. 2021;162(1).
5. Kang MH, Kim YJ, Lee JH. Mitochondria in reproduction. Clin Exp Reprod Med. 2023;50(1):1–11.
6. Hoque SAM, Kawai T, Zhu Z, Shimada M. Mitochondrial Protein Turnover Is Critical for Granulosa Cell Proliferation and Differentiation in Antral Follicles. J Endocr Soc. 2019;3(2):324–39.
7. Cecchino GN, Seli E, Alves da Motta EL, García-Velasco JA. The role of mitochondrial activity in female fertility and assisted reproductive technologies: overview and current insights. Reprod

Biomed Online. 2018;36(6):686–97.

8. Zhou J, Peng X, Mei S. Autophagy in Ovarian Follicular Development and Atresia. Int J Biol Sci. 2019;15(4):726–37.
9. Zou W, Ji D, Zhang Z, Yang L, Cao Y. Players in Mitochondrial Dynamics and Female Reproduction. Front Mol Biosci. 2021;8:717328.
10. Jornayvaz FR, Shulman GI. Regulation of mitochondrial biogenesis. Essays Biochem. 2010;47:69–84.
11. Chiaratti MR, Garcia BM, Carvalho KF, Macabelli CH, Ribeiro F, Zangirolamo AF, et al. Oocyte mitochondria: role on fertility and disease transmission. Anim Reprod. 2018;15(3):231–8.
12. Babayev E, Seli E. Oocyte mitochondrial function and reproduction. Curr Opin Obstet Gynecol. 2015;27(3):175–81.
13. Adhikari D, Lee IW, Yuen WS, Carroll J. Oocyte mitochondria-key regulators of oocyte function and potential therapeutic targets for improving fertility. Biol Reprod. 2022;106(2):366–77.
14. Warzych E, Lipinska P. Energy metabolism of follicular environment during oocyte growth and maturation. J Reprod Dev. 2020;66(1):1–7.
15. Kirillova A, Smitz JEJ, Sukhikh GT, Mazunin I. The Role of Mitochondria in Oocyte Maturation. Cells. 2021;10(9).
16. Chiaratti MR. Uncovering the important role of mitochondrial dynamics in oogenesis: impact on fertility and metabolic disorder transmission. Biophys Rev. 2021;13(6):967–81.
17. Kiriyama Y, Nochi H. Intra- and Intercellular Quality Control Mechanisms of Mitochondria. Cells. 2017;7(1).
18. Sharabi K, Lin H, Tavares CDJ, Dominy JE, Camporez JP, Perry RJ, et al. Selective Chemical Inhibition of PGC-1α Gluconeogenic Activity Ameliorates Type 2 Diabetes. Cell. 2017;169(1):148–e6015.
19. Lin H, Sharabi K, Lin L, Ruiz C, Zhu D, Cameron MD, et al. Structure-Activity Relationship and Biological Investigation of SR18292 (16), a Suppressor of Glucagon-Induced Glucose Production. J Med Chem. 2021;64(2):980–90.
20. Fabozzi G, Iussig B, Cimadomo D, Vaiarelli A, Maggiulli R, Ubaldi N et al. The Impact of Unbalanced Maternal Nutritional Intakes on Oocyte Mitochondrial Activity: Implications for Reproductive Function. Antioxid (Basel). 2021;10(1).
21. Li CJ, Lin LT, Tsui KH. Dehydroepiandrosterone Shifts Energy Metabolism to Increase Mitochondrial Biogenesis in Female Fertility with Advancing Age. Nutrients. 2021;13(7).
22. Ragonese F, Monarca L, De Luca A, Mancinelli L, Mariani M, Corbucci C, et al. Resveratrol depolarizes the membrane potential in human granulosa cells and promotes mitochondrial biogenesis. Fertil Steril. 2021;115(4):1063–73.
23. Jiang YF, Yu PH, Budi YP, Chiu CH, Fu CY. Dynamic changes in mitochondrial 3D structure during folliculogenesis and luteal formation in the goat large luteal cell lineage. Sci Rep. 2021;11(1):15564.

24. Budi YP, Hsu M-C, Lin Y-C, Lee Y-J, Chiu H-Y, Chiu C-H, et al. The injections of mitochondrial fusion promoter M1 during proestrus disrupt the progesterone secretion and the estrous cycle in the mouse. Sci Rep. 2023;13(1):2392.
25. Mutlu B, Puigserver P. GCN5 acetyltransferase in cellular energetic and metabolic processes. Biochim Biophys Acta Gene Regul Mech. 2021;1864(2):194626.
26. Cora MC, Kooistra L, Travlos G. Vaginal Cytology of the Laboratory Rat and Mouse:Review and Criteria for the Staging of the Estrous Cycle Using Stained Vaginal Smears. Toxicol Pathol. 2015;43(6):776–93.
27. Quignon C. Collection and Analysis of Vaginal Smears to Assess Reproductive Stage in Mice. Curr Protoc. 2023;3(9):e887.
28. McLean AC, Valenzuela N, Fai S, Bennett SA. Performing vaginal lavage, crystal violet staining, and vaginal cytological evaluation for mouse estrous cycle staging identification. J Vis Exp. 2012(67):e4389.
29. Taft R. In Vitro Fertilization in Mice. Cold Spring Harb Protoc. 2017;2017(11):pdb.prot094508
30. Ewels P, Magnusson M, Lundin S, Käller M. MultiQC: summarize analysis results for multiple tools and samples in a single report. Bioinformatics. 2016;32(19):3047–8.
31. Bolger AM, Lohse M, Usadel B. Trimmomatic: a flexible trimmer for Illumina sequence data. Bioinformatics. 2014;30(15):2114–20.
32. Kim D, Langmead B, Salzberg SL. HISAT: a fast spliced aligner with low memory requirements. Nat Methods. 2015;12(4):357–60.
33. Sahraeian SME, Mohiyuddin M, Sebra R, Tilgner H, Afshar PT, Au KF, et al. Gaining comprehensive biological insight into the transcriptome by performing a broad-spectrum RNA-seq analysis. Nat Commun. 2017;8(1):59.
34. Love MI, Huber W, Anders S. Moderated estimation of fold change and dispersion for RNA-seq data with DESeq2. Genome Biol. 2014;15(12):550.
35. Schurch NJ, Schofield P, Gierliński M, Cole C, Sherstnev A, Singh V, et al. How many biological replicates are needed in an RNA-seq experiment and which differential expression tool should you use? RNA. 2016;22(6):839–51.
36. Kanehisa M, Araki M, Goto S, Hattori M, Hirakawa M, Itoh M, et al. KEGG for linking genomes to life and the environment. Nucleic Acids Res. 2008;36(Database issue):D480–4.
37. Kanehisa M, Sato Y, Furumichi M, Morishima K, Tanabe M. New approach for understanding genome variations in KEGG. Nucleic Acids Res. 2019;47(D1):D590–5.
38. Yu G, Wang LG, Han Y, He QY. clusterProfiler: an R package for comparing biological themes among gene clusters. Omics. 2012;16(5):284–7.
39. Subramanian A, Tamayo P, Mootha VK, Mukherjee S, Ebert BL, Gillette MA, et al. Gene set enrichment analysis: a knowledge-based approach for interpreting genome-wide expression profiles. Proc Natl Acad Sci U S A. 2005;102(43):15545–50.

40. Wang T, Xu P, Yuan J, Chen H, Guo X, Gao J, et al. Mitochondrial dysfunction in oocytes: implications for fertility and ageing. J Ovarian Res. 2025;18(1):186.
41. Yazawa T, Inaoka Y, Okada R, Mizutani T, Yamazaki Y, Usami Y, et al. PPAR-gamma coactivator-1alpha regulates progesterone production in ovarian granulosa cells with SF-1 and LRH-1. Mol Endocrinol. 2010;24(3):485–96.
42. Yang Z, Liu S, Pan X. Research progress on mitochondrial damage and repairing in oocytes: A review. Mitochondrion. 2024;75:101845.
43. May-Panloup P, Boucret L, de la Chao JM, Desquiret-Dumas V, Ferré-L'Hotellier V, Morinière C, et al. Ovarian ageing: the role of mitochondria in oocytes and follicles. Hum Reprod Update. 2016;22(6):725–43.
44. Hao X, Zhao J, Rodriguez-Wallberg KA. Comprehensive atlas of mitochondrial distribution and dynamics during oocyte maturation in mouse models. Biomark Res. 2024;12(1):125.
45. Bahety D, Böke E, Rodríguez-Nuevo A. Mitochondrial morphology, distribution and activity during oocyte development. Trends Endocrinol Metab. 2024;35(10):902–17.
46. Zhang X, Wu XQ, Lu S, Guo YL, Ma X. Deficit of mitochondria-derived ATP during oxidative stress impairs mouse MII oocyte spindles. Cell Res. 2006;16(10):841–50.
47. Li G, Gu J, Zhou X, Wu T, Li X, Hua R, et al. Mitochondrial stress response gene Clpp deficiency impairs oocyte competence and deteriorate cyclophosphamide-induced ovarian damage in young mice. Front Endocrinol (Lausanne). 2023;14:1122012.
48. Nazir F, Baibrus MA, Tariq M, Tharwat M, Pei S, Wen Y, et al. Integrated Multi-Omics Reveals Disruption of Lipid–Steroid Regulatory Axis Underlying Chronic Heat Stress-Induced Ovarian Dysfunction in Mice. Int J Mol Sci. 2026;27(19):8671.
49. Lucki NC, Sewer MB. Multiple roles for sphingolipids in steroid hormone biosynthesis. Subcell Biochem. 2008;49:387–412.
50. Kamar Bashah NA, Hamid AA, Adam SH, Jaffar FHF, Abd Rahman IZ, Mokhtar MH. Role of AMP-Activated Protein Kinase (AMPK) in Female Reproduction: A Review. Int J Mol Sci. 2025;26(14).
51. Yang W, Wang L, Wang F, Yuan S. Roles of AMP-Activated Protein Kinase (AMPK) in Mammalian Reproduction. Front Cell Dev Biol. 2020;8:593005.
52. Bakhshalizadeh S, Amidi F, Shirazi R, Shabani Nashtaei M. Vitamin D3 regulates steroidogenesis in granulosa cells through AMP-activated protein kinase (AMPK) activation in a mouse model of polycystic ovary syndrome. Cell Biochem Funct. 2018;36(4):183–93.
53. Zhan X, Luo P, Yang Y, Deng Z, Zhang C, Yang C, et al. AMPK/ULK1 enhances mitophagy and steroidogenesis in duck Granulosa cells under heat exposure. Poult Sci. 2026;105(9):107189.
54. Childs GV, Odle AK, MacNicol MC, MacNicol AM. The Importance of Leptin to Reproduction. Endocrinology. 2021;162(2).
55. Anaya ES, de Groot EL, Lydon JP, Pangas SA, Hartig SM. Contributions of white adipose tissue to energy requirements for female reproduction. Trends Endocrinol Metab. 2024;35(9):809–20.

56. Adamowski M, Sharma Y, Molcan T, Wołodko K, Kelsey G, Galvão AM. Leptin signalling regulates transcriptional differences in granulosa cells from genetically obese mice but not the activation of NLRP3 inflammasome. Sci Rep. 2024;14(1):8070.
57. Spicer LJ, Francisco CC. The adipose obese gene product, leptin: evidence of a direct inhibitory role in ovarian function. Endocrinology. 1997;138(8):3374–9.
58. Cioffi JA, Van Blerkom J, Antczak M, Shafer A, Wittmer S, Snodgrass HR. The expression of leptin and its receptors in pre-ovulatory human follicles. Mol Hum Reprod. 1997;3(6):467–72.
59. Zhang D, Wang F, Li P, Gao Y. Mitochondrial Ca(2+) Homeostasis: Emerging Roles and Clinical Significance in Cardiac Remodeling. Int J Mol Sci. 2022;23(6).
60. Chen C, Huang Z, Dong S, Ding M, Li J, Wang M, et al. Calcium signaling in oocyte quality and functionality and its application. Front Endocrinol (Lausanne). 2024;15:1411000.
61. Miao YL, Williams CJ. Calcium signaling in mammalian egg activation and embryo development: the influence of subcellular localization. Mol Reprod Dev. 2012;79(11):742–56.
62. Rong S, Fu Y, Li Y, Jiang YC, Chen L, Zhao Y et al. Metabolic regulation of oocyte maturation and early embryo development in mammals. Life Metabolism. 2026;5(6).

Figures

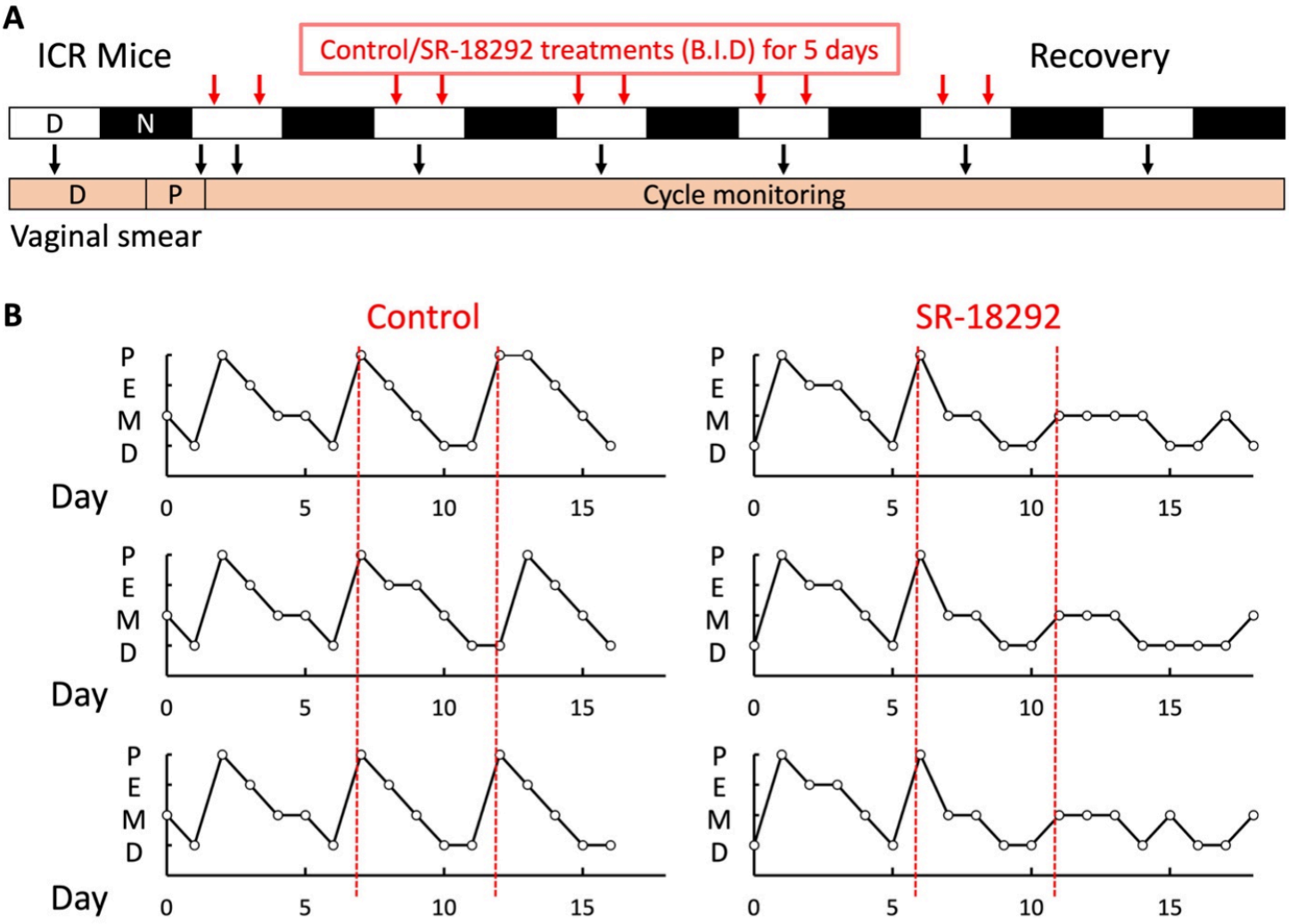


Figure 1

Cycle monitoring during SR-18292 treatment. (A) The experimental design and procedure of the study. (B) Daily vaginal smears were collected from control and SR-18292-treated mice before, during, and after the 5-day treatment period (red vertical dotted lines) to monitor estrous cyclicity. Each data point represents one vaginal smear collection. *n*=3/group. ±: with or without SR-18292. D: day, N: night, D: diestrus, P: proestrus, E: estrus, and M: metestrus

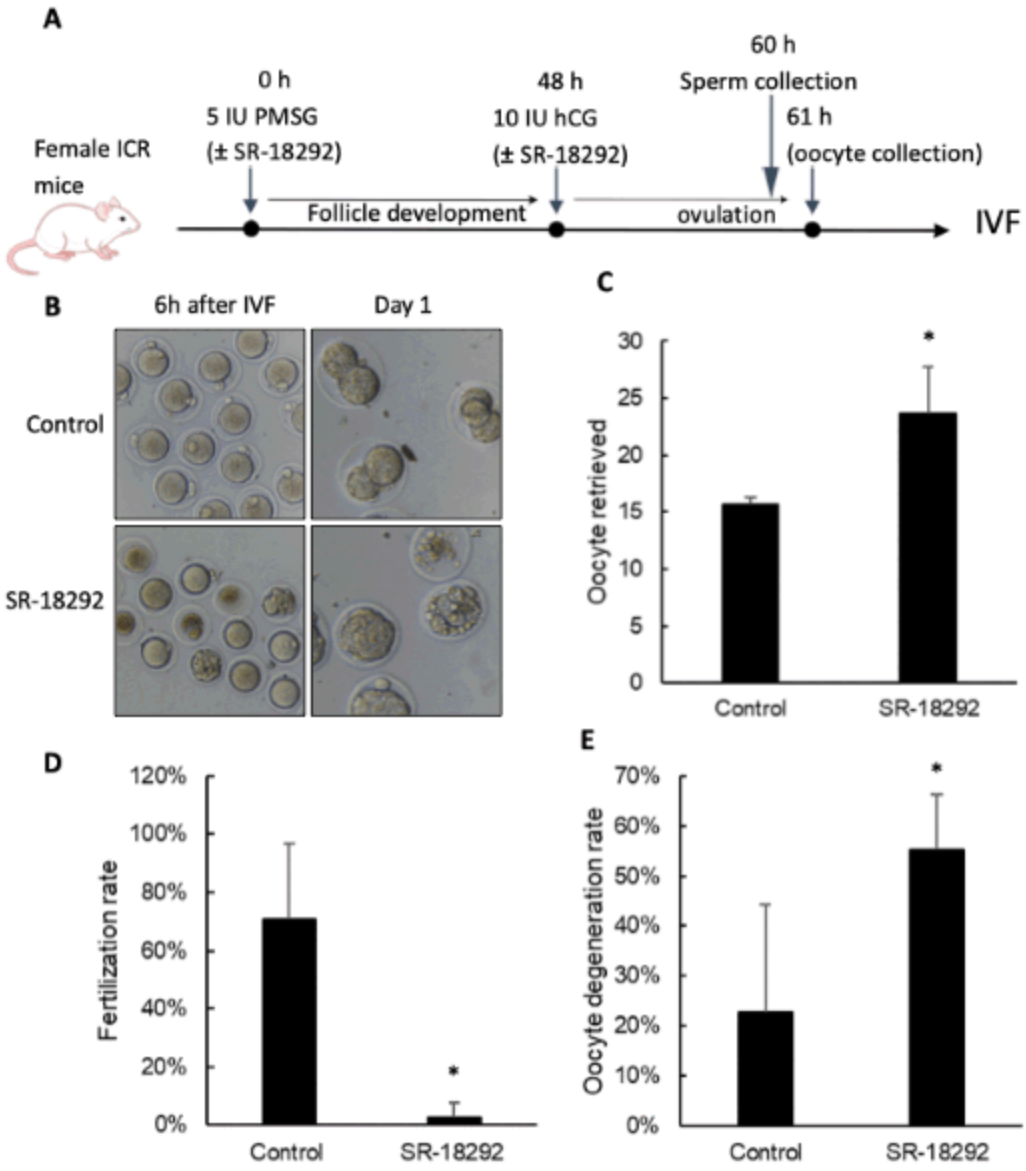


Figure 2

Effects of SR-18292 Treatment on In Vitro Fertilization Outcomes in Mice. (A) Schematic of mouse superovulation procedure and experimental groups. (B) The representative images show the embryos after IVF. (C) The number of oocytes retrieved after superovulation. (D) The fertilization rate of oocytes after SR-18292 treatment. (E) The rate of oocyte degeneration after 6 hours of IVF. The data are presented as Mean ± SD, * indicating a significant difference (compared to the control group, Student's t-test, $p<0.05$). The mouse illustration was created with ChatGPT (OpenAI).

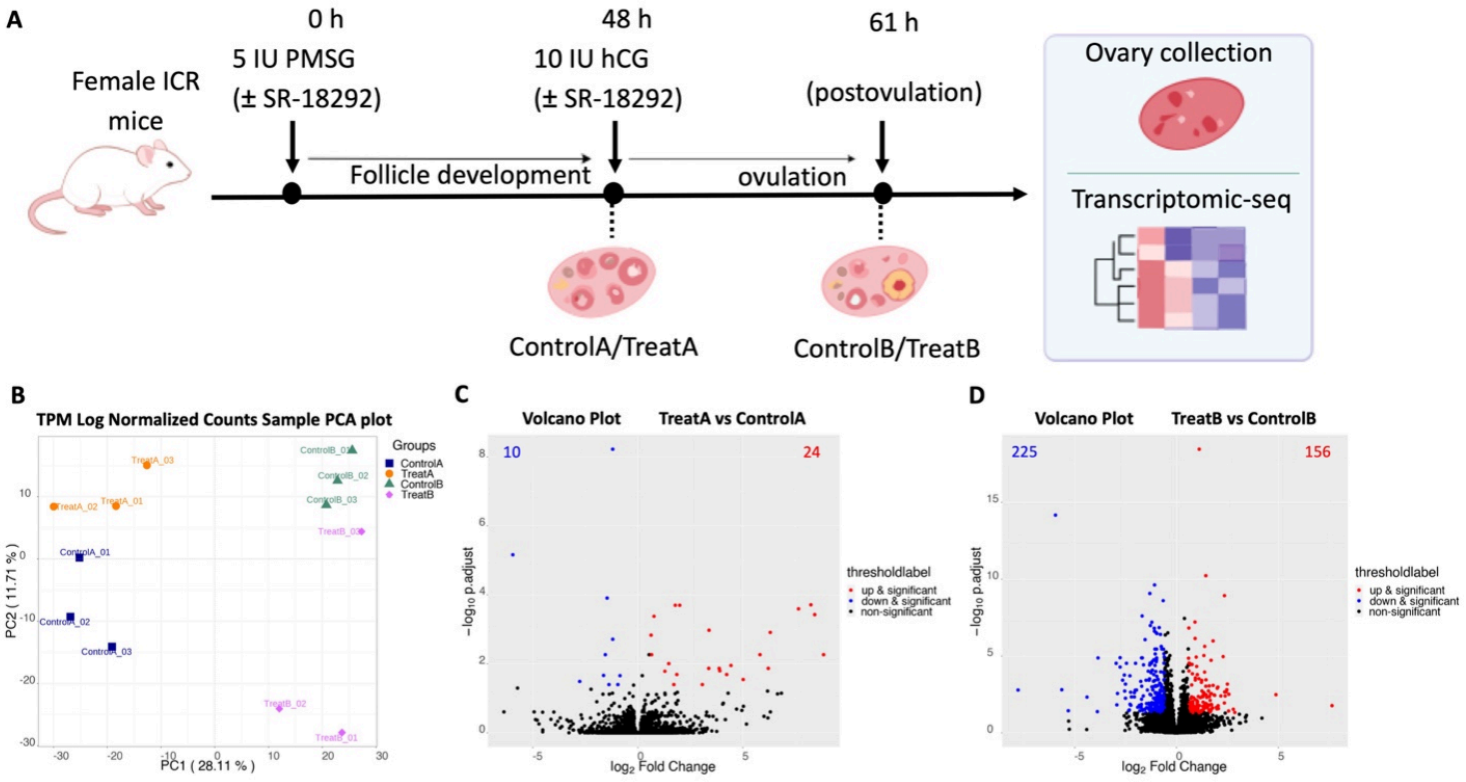


Figure 3

RNA-sequencing design and DEG analysis. (A) Experimental layout showing treatment and sampling time points on ~ 5-week-old mice. Sampling points represent retrieval of blood and ovarian tissue from mice. The schematic illustration was created with assistance from ChatGPT(OpenAI). (B) Principal component analysis (PCA) plot showing the distribution pattern of samples in the control and treatment groups. Each group has its own representative color code and shape. (C, D) Volcano plot indicating RNA-seq comparison between treatment and control groups. Blue dots represent down-regulated differentially expressed genes (DEGs) in treated mice; red dots represent upregulated genes in treated mice; black dots represent non-significantly regulated genes. (C) TreatA compared to ControlA; (D) TreatB compared to ControlB. DEG analysis filter parameters: *p*-adjust, fold change >1.5. ±: indicating with or without SR-18292; PMSG: pregnant mare serum gonadotropin; hCG: human chorionic gonadotropin. *n*= 3mice/group

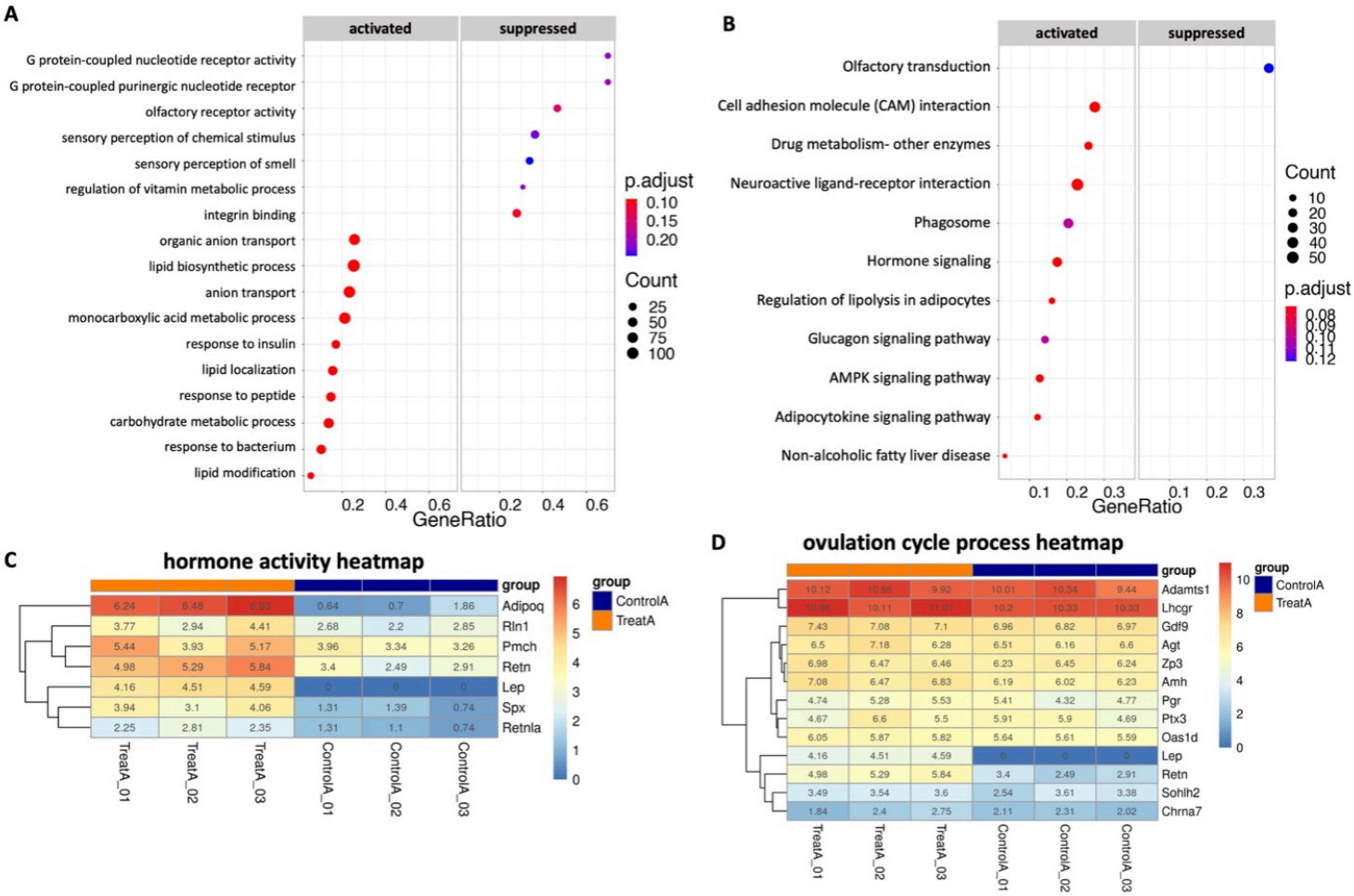


Figure 4

Early SR-18292 exposure alters ovarian pathways associated with hormonal activity and ovulation in mice. (A, B) Gene set enrichment analysis (GSEA) dot plots showing the top 10 enriched pathways in approximately 5-week-old SR-18292-treated mice (TreatA) relative to controls (ControlA), categorized as activated or suppressed. Dot color represents the adjusted *P*-value, and dot size indicates the number of genes associated with each pathway. (C, D) Heatmaps of GSEA-associated gene expression patterns in TreatA and ControlA mice for (C) hormone activity and (D) ovulation cycle processes. Heatmap colors range from blue to red, representing lower to higher gene expression, respectively. *n* = 3 mice per group.

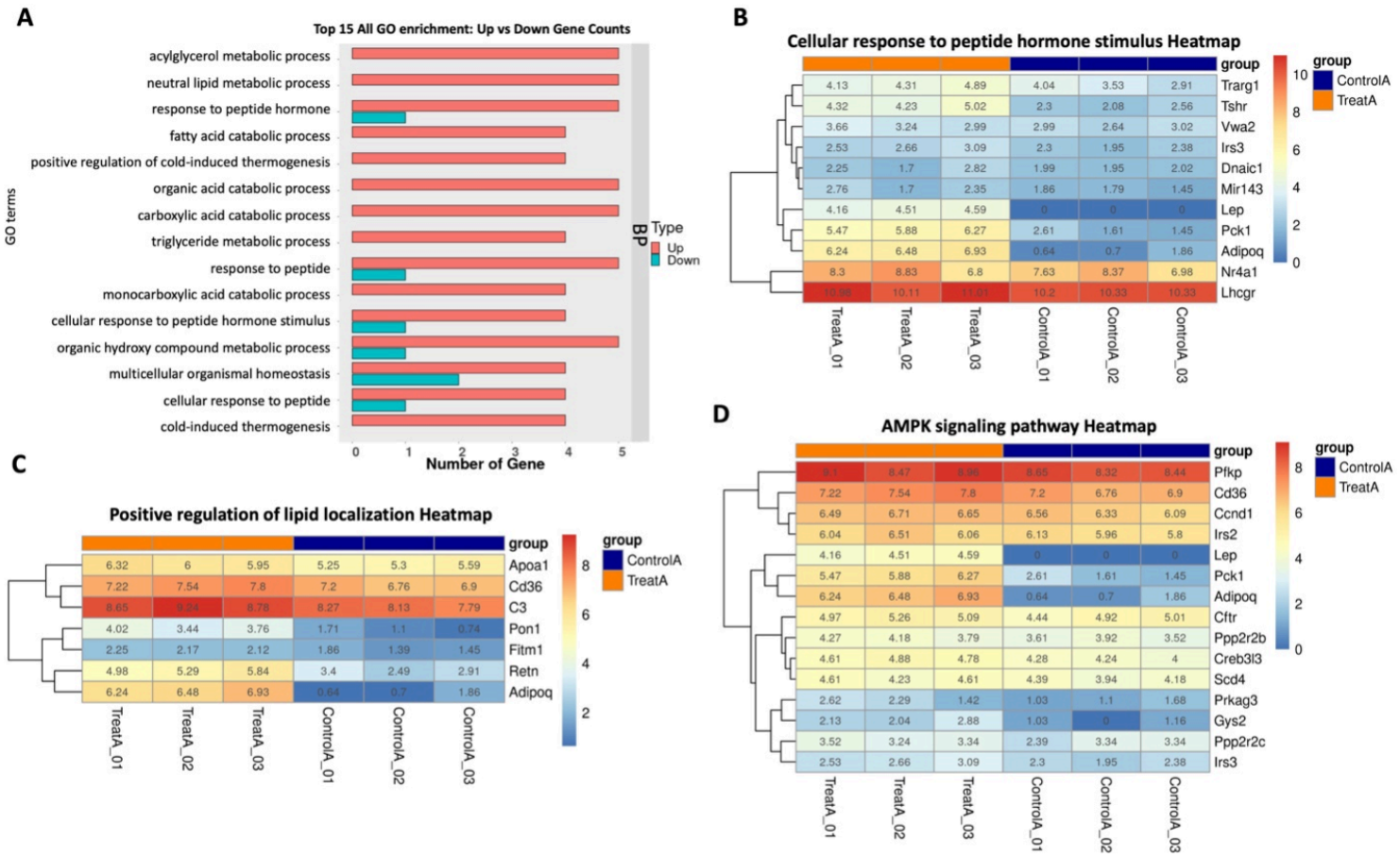


Figure 5

Compensatory transcriptional pathways associated with the maintenance of ovarian function following SR-18292 exposure. (A) GO enrichment analysis showing the top 15 upregulated and downregulated biological processes (BP) in TreatA mice relative to ControlA mice. Bars represent the number of differentially expressed genes (DEGs) associated with each term. Differential expression was defined using an adjusted *P*-value threshold and a fold change greater than 1.5. (B–D) Heatmaps showing gene expression patterns associated with selected GSEA pathways in TreatA and ControlA mice. Orange and blue indicate TreatA and ControlA groups, respectively. (B) Cellular response to peptide hormone stimulus; (C) positive regulation of lipid localization; and (D) AMPK signaling pathway. The blue-to-red color gradient represents low-to-high gene expression levels, respectively. *n*= 3 mice per group.

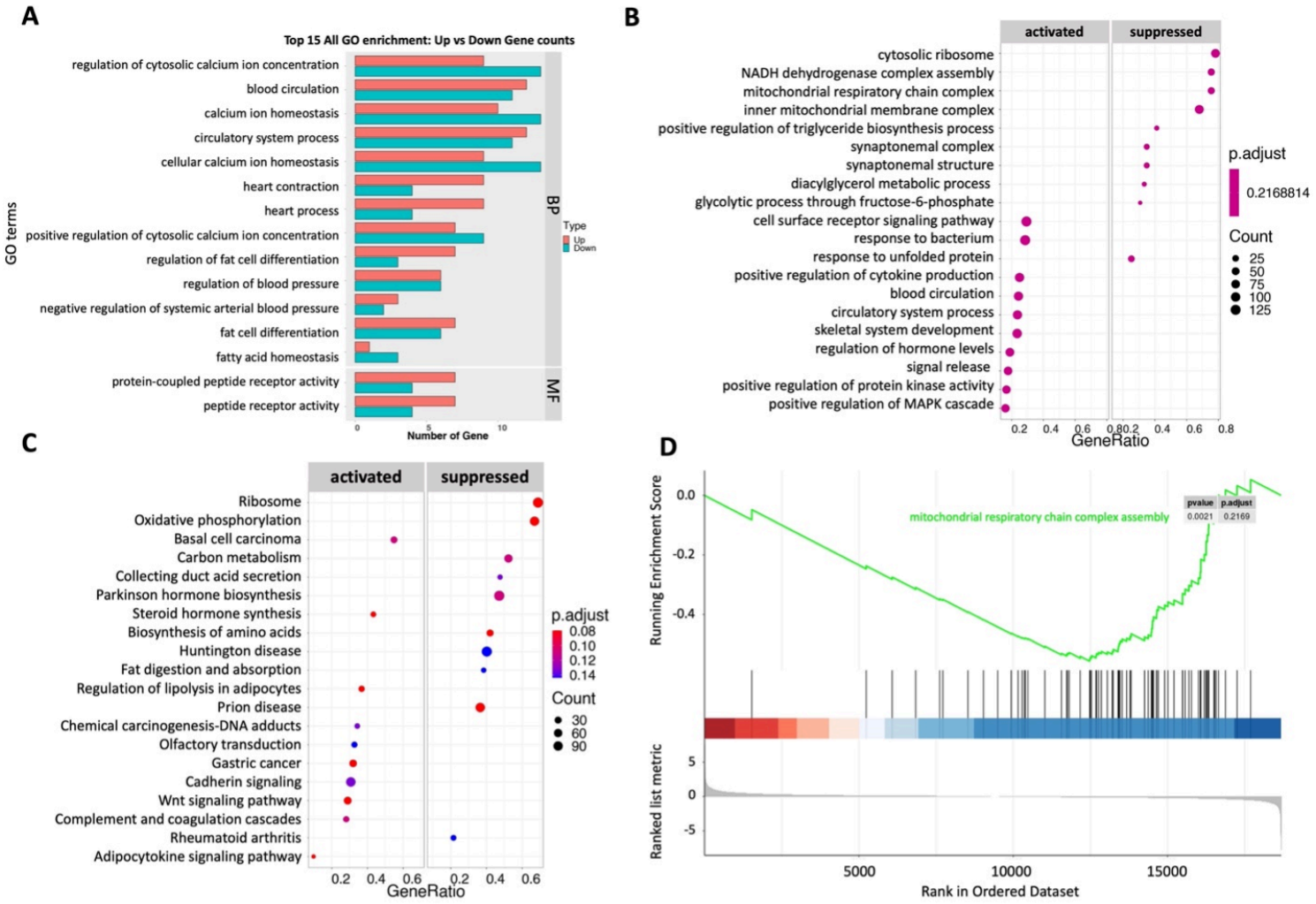


Figure 6

SR-18292 alters ovarian transcriptional pathways following superovulation. (A) GO enrichment analysis showing the top 15 upregulated and downregulated terms within the molecular function (MF) and biological process (BP) categories in TreatB mice relative to ControlB mice. Bars represent the number of differentially expressed genes (DEGs) associated with each GO term. The selection criteria included an adjusted *P*-value threshold and a fold-change cutoff of 1.5. (B, C) GSEA dot plots showing the top 10 positively and negatively enriched pathways in TreatB mice compared with ControlB mice. Dot color represents the adjusted *P*-value, and dot size indicates the number of genes associated with each pathway. (B) GO pathway analysis; (C) KEGG pathway analysis. (D) GSEA enrichment plot showing negative enrichment of the mitochondrial respiratory chain complex assembly gene set in TreatB mice relative to ControlB mice, with the enrichment signal concentrated toward the right side of the ranked gene list.

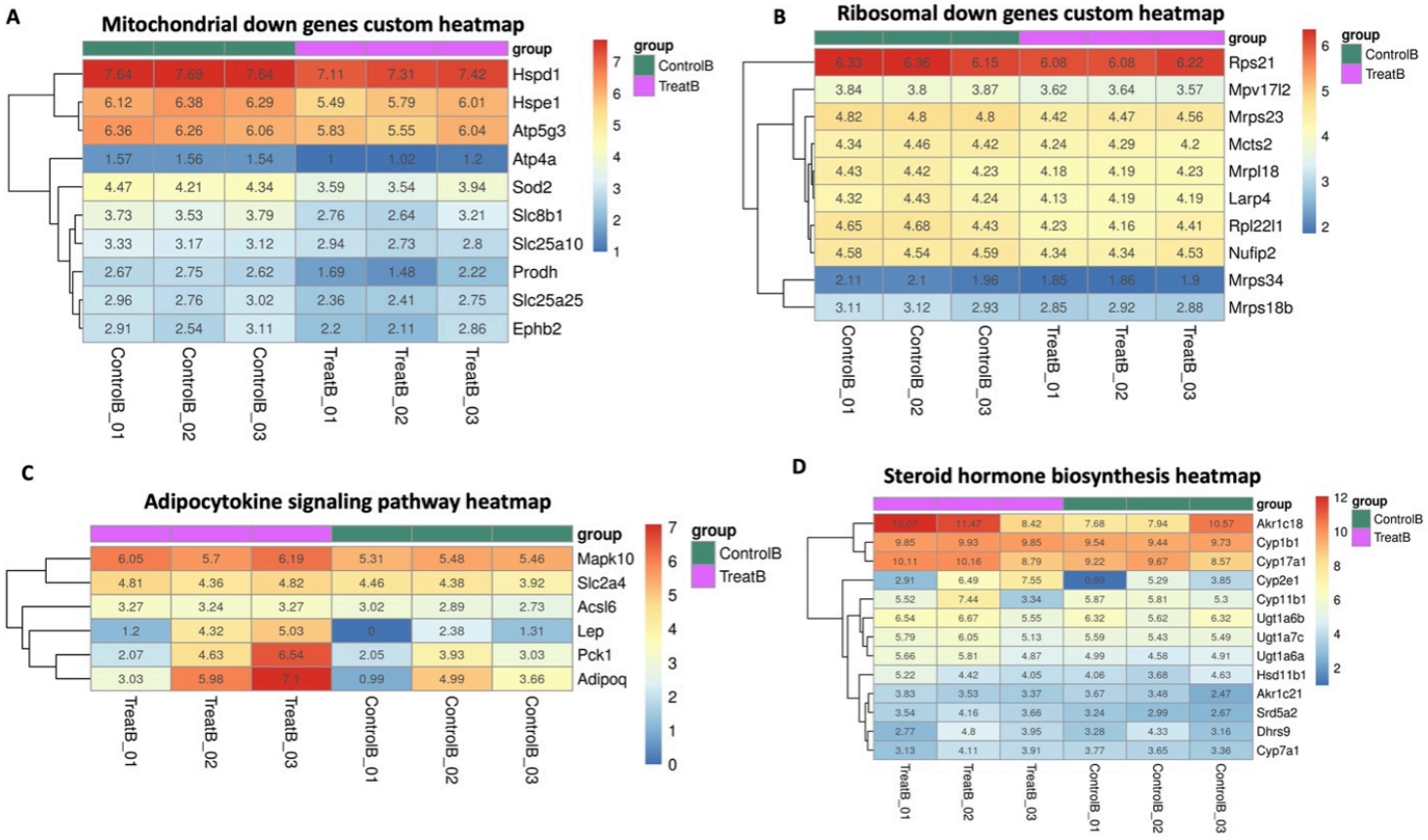


Figure 7

Differential expression of mitochondrial, ribosomal, and compensatory pathway-associated genes following SR-18292 treatment. Custom heatmaps showing representative downregulated genes associated with (A) mitochondrial function and (B) ribosomal function in TreatB mice compared with ControlB mice. (C, D) GSEA heatmaps showing positively enriched gene sets associated with (C) adipocytokine signaling and (D) steroid hormone biosynthesis in TreatB mice relative to ControlB mice. The blue-to-red color gradient represents low-to-high gene expression levels, respectively. Green indicates genes upregulated in TreatB mice relative to ControlB mice.

Supplementary Files

This is a list of supplementary files associated with this preprint. Click to download.

- SR18292Supplementarydata.docx